

Journal of Prime Research in Mathematics



Stochastic Differential Equations based on Perona-Malik Functions for Image denoising

Radhia Halilou^{a,*}, Fatma Zohra Nouri^a

^a Mathematical Modeling and Numerical Simulation Laboratory, Faculty of Sciences, Badji Mokhtar University, P.O. Box 12, Annaba 23000-Algeria.

Abstract

The aim of this work is to propose models based on stochastic differential equations with a good choice for both diffusion and drift terms to solve an image restoration problem. These proposed models are based on Barbu and Borkowski stochastic equations, where we exploit the Perona-Malik functions for the drift and diffusion terms. First, we show the derived model's well posedness; then we present the related numerical results. These models give satisfactory experimental results in removing noise, improving and preserving the image structure compare to other well known approaches, such as [1], [2] and [4].

Keywords: Stochastic Differential Equations, Analysis and Well-Posedness, Numerical Methods, Image

Processing.

2010 MSC: 65C30, 60H35, 65R10, 94A08.

1. Introduction

Many techniques have been used for image processing, for example in a transform domain, we have Fourier analysis [21], [23] and [24], and wavelets [10] and [11], where they contain numerous recent methods such as block matching 3D (BM3D) [7] and [13]. In addition, several special domain methods among them total variation [11], [16] and [17], partial differential equations (PDEs) [14],[15], [25], [27] and [26]. Most of these methods have limitations such as ill-posedness [20] and [18], blurred image, or loss of important features (edges, contours, .. etc); which make it harder to identify the image details [15]. In the 20th century, PDEs were very successful in restoring images, especially the Perona-Malik (PM) [20] model, which does not only remove the noise but also preserves the edges, though it is ill-posed [18]. Recently, a new research in image processing based on stochastic differential equations (SDEs) [1], [2], [4], [5], [6], [8] and [9], has been developed since there is a relationship between the SDEs and PDEs [22], leading to better results. The relationship between SDEs and PDEs is the probabilistic approach of a PDE that allows expressing their

^{*}Halilou Radhia

Email addresses: radhia.halilou@univ-annaba.dz (Radhia Halilou), fatma-zohra.nouri@univ-annaba.dz (Fatma Zohra Nouri)

solutions in the form of the expectation of a certain function of a stochastic process. Furthermore, according to Itô and Kolmogorov formula [12] and [19], we can move from one to another.

In this work, we first highlight two types of SDEs to image enhancement, one was introduced by Barbu et al [2], where the authors set the diffusion to 1 and the other by Borkowski et al [4] who neglected the drift term. Based on these two SDEs, we propose a model, combining drift and diffusion terms from Barbu and Borkowski SDEs together with PM functions [20]. We start by showing the well-posedness of the derived models, then we proceed to their discretisations by finite difference schemes. A comparative study leads us to show how the obtained numerical results are very satisfactory and encouraging, in denoising and contour preserving.

The paper is structured as follows: Section 2 provides an overview of related work on stochastic differential equations. In Section 3, we present the proposed models, exploring various configurations of the drift and diffusion terms. Section 4 focusses on the description of numerical discretisation techniques and discussions of the obtained results. Finally, concluding remarks are presented in Section 5.

2. Recent related work on SDEs

In this section, we present briefly some related results.

2.1. Barbu's model

Barbu et al in [2] have proposed the following stochastic model

$$\begin{cases}
 dX(t) = \underbrace{\mu(X(t))}_{drift} dt + dW(t), \\
 X(0, x, y) = X_0(x, y) \in \mathbb{R}^2,
\end{cases}$$
(2.1)

where $X(t): \mathbb{R}^2 \longrightarrow \mathbb{R}^2$ is the diffusion process, $W(t) = \lambda \{\omega_1(t), \omega_2(t)\}, \lambda \in (0, 1)$, represents a 2D Brownian motion in a probability space $\{\Omega, F, P\}$ with the natural filtration $(F_t)_{t\geq 0}$. The drift term $\mu: \mathbb{R}^2 \longrightarrow \mathbb{R}^2$ is Lipschitzian defined by

$$\mu(X(t)) = -\left(e^{-\alpha_1|X(t)|^2}, e^{-\alpha_2|X(t)|^2}\right),\tag{2.2}$$

with $\alpha_1, \alpha_2 \geq 0$, $X(t) = \{X_1(t), X_2(t)\}$ represents a random variable, where: $|X(t)|^2 = X_1(t)^2 + X_2(t)^2$ and $X_0(x, y) \in \mathbb{R}^2$ is the position of the pixel (x, y) in the initial image.

2.2. Borkowski's model

Borkowski et al in [4] proposed the following SDE

$$\begin{cases}
 dX(t) = \underbrace{\sigma(X(t))}_{diffusion} dW(t), \\
 X(0, x, y) = X_0(x, y) \in \mathbb{R}^2,
\end{cases}$$
(2.3)

where $\sigma(X(t))$ is defined as

$$\sigma(X(t)) = \begin{pmatrix} -\frac{(G_{\gamma} * u_0)_y(X(t))}{|\nabla(G_{\gamma} * u_0)(X(t))|} & 0\\ \frac{(G_{\gamma} * u_0)_x(X(t))}{|\nabla(G_{\gamma} * u_0)(X(t))|} & 0 \end{pmatrix},$$
(2.4)

with $(G_{\gamma} * u_0)_y = \frac{\partial (G_{\gamma} * u_0)}{\partial y}$, $(G_{\gamma} * u_0)_x = \frac{\partial (G_{\gamma} * u_0)}{\partial x}$. Here G_{γ} denotes the Gaussian (smoothing) filter such that $G_{\gamma}(x,y) = \frac{1}{2\pi\gamma^2}e^{-\frac{(x^2+y^2)}{2\gamma^2}}$

3. Proposed Model 1

Here, we propose to combine Barbu's drift (2.2) and Borkowski's diffusion (2.4) to get

$$\begin{cases}
 dX(t) = \underbrace{\mu(X(t))}_{drift} dt + \underbrace{\sigma(X(t))}_{diffusion} dW_t, \\
 X(0, x, y) = X_0(x, y) \in \mathbb{R}^2,
\end{cases}$$
(3.1)

where X(t) is the stochastic process and the associated solution is given by

$$X(t) = X_0 + \int_0^t \mu(X(s))ds + \int_0^t \sigma(X(s))dW(s).$$
 (3.2)

The restored image is defined by

$$u(x,y) = E[u_0(X_T)] = \frac{1}{M} \sum_{i=1}^{M} u_0(X_T^m(\beta_i)), \tag{3.3}$$

where $X_T^m(\beta_i)$ is the stochastic process's trajectory approximation of X(t), with m, T and β_i denote the m^{th} iteration, the final time and the random variable, respectively, whereas the number of Monte Carlo iterations is represented by M and $u_0 : \mathbb{R}^2 \to \mathbb{R}$, the noisy image.

3.1. Mathematical analysis

3.1.1. Existence and Uniqueness

In this section, we study the well-posedness of (3.1). We set the following results for the existence and uniqueness of the associated solution.

Theorem 3.1. (B.Øksendal, [19]) Let $t \in [0,T]$, and $\{w_t\}_{t\geq 0}$ be a d-dimensional Brownian motion on a probability space (Ω, F, P) with natural filtration $\{F_t\}_{t\geq 0}$. We have the SDE (3.1), where μ and σ are measurable defined by

$$\mu: [0,T] \times \mathbb{R}^d \to \mathbb{R}^d \text{ and } \sigma: [0,T] \times \mathbb{R}^d \to \mathbb{R}^{d \times d'} \text{ (where } |\sigma|^2 = \sum |\sigma_{i,j}|^2).$$

If μ and σ satisfy the Lipschitz and linear growth conditions, respectively i.e.

$$|\mu(t,X) - \mu(t,Y)| + |\sigma(t,X) - \sigma(t,Y)| \le M_1|X - Y|,$$
 (3.4)

$$t \in [0, T], \forall X, Y \in \mathbb{R}^d$$

$$|\mu(t, X)| + |\sigma(t, X)| \le M_2(1 + |X|),$$

$$t \in [0, T], \forall X, Y \in \mathbb{R}^d$$

$$(3.5)$$

for some constant M_1 and M_2 . Let $X_0 = Y$ be a random variable independent of the σ -algebra $F_{\infty}^{(m)}$ adapted by $\{w_s\}_{s \leq t}$ and verify $E\left[|Y|^2\right] < \infty$. Then (3.1) has a unique solution X(t), where

$$E\left[\int_0^T |X(t)|^2 dt\right] < \infty$$

and X(t) adapted by the filtration F_t^Y .

Note that

• $F_{\infty}^{(m)}$ is the σ -algebra generated by the m-dimensional Brownian motion $\{w_s\}_{s\leq t}$

• F_t^Y is the filtration generated by the initial condition Y and the Brownian motion $\{w_s\}_{s \leq t}$.

Let us adapt this result in the proposed model, i.e. (3.1) together with (2.2) and (2.4).

Theorem 3.2. If functions (2.2) and (2.4) verify (3.4) and (3.5), then there exists a unique solution to (3.1).

To prove this theorem, we first prove the two following propositions.

Proposition 3.3. Let $\mu(.,.)$ and $\sigma(.,.)$ defined by (2.2) and (2.4), respectively, be measurable functions on $[0,T] \times \mathbb{R}^2$, and |.| be an Euclidean norm. Then we have

$$|\mu(t,X)| + |\sigma(t,X)| \le M_1(1+|X|),$$
(3.6)

with $M_1 > 0$ is the linear growth constant.

Proof. If we use (2.2) and (2.4) for μ and σ , respectively, we get

$$|\mu(t,X)|^{2} = \left(e^{-\alpha_{1}|X|^{2}}\right)^{2} + \left(e^{-\alpha_{2}|X|^{2}}\right)^{2}$$

$$= e^{-2\alpha_{1}|X|^{2}} + e^{-2\alpha_{2}|X|^{2}},$$

$$\leq 2\alpha_{1}|X|^{2} + 2\alpha_{2}|X|^{2},$$

$$= 2(\alpha_{1} + \alpha_{2})|X|^{2},$$

$$\leq 4\alpha|X|^{2}, \ \forall \alpha_{1}, \alpha_{2} > 0, X \in \mathbb{R}^{2}, \ t \in [0,T],$$

with $\alpha = max(\alpha_1, \alpha_2)$. Hence

$$|\mu(t,X)| \le 2\sqrt{\alpha}|X| + 2\sqrt{\alpha} \le 2\sqrt{\alpha}(1+|X|). \tag{3.7}$$

If we put $(G_{\gamma} * u_0)(X) = F(X)$, we can write

$$|\sigma(t,X)|^{2} = \left(-\frac{F_{y}(X)}{|\nabla F(X)|}\right)^{2} + \left(\frac{F_{x}(X)}{|\nabla F(X)|}\right)^{2}$$

$$= \frac{(F_{y}(X))^{2}}{(F_{x}(X))^{2} + (F_{y}(X))^{2}} + \frac{(F_{x}(X))^{2}}{(F_{x}(X))^{2} + (F_{y}(X))^{2}}$$

$$= \frac{(F_{y}(X))^{2} + (F_{x}(X))^{2}}{(F_{x}(X))^{2} + (F_{y}(X))^{2}}$$

$$= 1.$$

Hence

$$|\sigma(t,X)| \le 1 + |X|, \forall X \in \mathbb{R}^2. \tag{3.8}$$

From (3.7) and (3.8) we obtain

$$|\mu(t,X)| + |\sigma(t,X)| \le 2\sqrt{\alpha}(1+|X|) + (1+|X|)$$
 (3.9)

$$= (2\sqrt{\alpha} + 1)(1 + |X|) \tag{3.10}$$

$$\leq M_1(1+|X|),$$
 (3.11)

with $M_1 = 2\sqrt{\alpha} + 1$.

This proves proposition 3.3.

Proposition 3.4. Let μ and σ be defined by (2.2) and (2.4), then

$$|\mu(t,X) - \mu(t,Y)| + |\sigma(t,X) - \sigma(t,Y)| \le M_2 |X - Y|,$$
 (3.12)

with $M_2 > 0$ is the Lipschitz constant.

Proof. In the same way we use (2.2) and (2.4) for μ and σ , respectively and get

$$\begin{aligned} |\mu(t,X) - \mu(t,Y)|^2 &= \left(e^{-\alpha_1|X|^2} - e^{-\alpha_1|Y|^2}\right)^2 + \left(e^{-\alpha_2|X|^2} - e^{-\alpha_2|Y|^2}\right)^2 \\ &\leq \alpha_1|X|^2 - \alpha_1|Y|^2 + \alpha_2|X|^2 - \alpha_2|Y|^2 \\ &= (\alpha_1 + \alpha_2)|X|^2 - (\alpha_1 + \alpha_2)|Y|^2 \\ &= (\alpha_1 + \alpha_2)(|X|^2 - |Y|^2) \\ &\leq 4\alpha \left(|X| - |Y|\right) \left(|X| + |Y|\right) \\ &\leq 4\alpha K \left(|X - Y|\right), \end{aligned}$$

with $\alpha = max(\alpha_1, \alpha_2) > 0$, and K = |X| + |Y|.

Hence

$$|\mu(t,X) - \mu(t,Y)| \le 2\sqrt{\alpha K}|X - Y|. \tag{3.13}$$

$$|\sigma(t,X) - \sigma(t,Y)|^{2} = \left(-\frac{F_{y}(X)}{|\nabla F(X)|} + \frac{F_{y}(Y)}{|\nabla F(Y)|}\right)^{2} + \left(\frac{F_{x}(X)}{|\nabla F(X)|} - \frac{F_{x}(Y)}{|\nabla F(Y)|}\right)^{2}$$

$$= \left(\frac{F_{y}(X)}{|\nabla F(X)|}\right)^{2} + \left(\frac{F_{y}(Y)}{|\nabla F(Y)|}\right)^{2} - 2\frac{F_{y}(X)}{|\nabla F(X)|} \cdot \frac{F_{y}(Y)}{|\nabla F(Y)|}$$

$$+ \left(\frac{F_{x}(X)}{|\nabla F(X)|}\right)^{2} + \left(\frac{F_{x}(Y)}{|\nabla F(Y)|}\right)^{2} - 2\frac{F_{x}(X)}{|\nabla F(X)|} \cdot \frac{F_{x}(Y)}{|\nabla F(Y)|}$$

$$\leq (F_{y}(X))^{2} + (F_{y}(Y))^{2} + (F_{x}(X))^{2} + (F_{x}(Y))^{2}$$

$$-2(F_{y}(X)F_{y}(Y)) - 2(F_{x}(X)F_{x}(Y))$$

$$\leq (\nabla F(X))^{2} + (\nabla F(Y))^{2} - 2(\nabla F(X)\nabla F(Y))$$

$$= (\nabla F(X) - \nabla F(Y))^{2}. \tag{3.14}$$

For a given differentiable function F(X) within a convex set, there exists a positive constant L such that (3.14) can be formulated as

$$|\sigma(t,X) - \sigma(t,Y)| \le L|X - Y|,\tag{3.15}$$

with L > 0 is the Lipschitz constant.

From (3.13) and (3.15) we obtain,

$$|\mu(t,X) - \mu(t,Y)| + |\sigma(t,X) - \sigma(t,Y)| \le 2\sqrt{\alpha K}|X - Y| + L|X - Y|$$

 $\le M_2|X - Y|,$ (3.16)

with
$$M_2 = 2\sqrt{\alpha K} + L$$
.

From the two propositions 3.3 and 3.4, we conclude that the proposed model has a unique solution.

3.2. Proposed Model 2

SDEs with **Perona-Malik functions**.

We choose drift and diffusion terms as follows:

1. We consider (3.1) with PM functions as drift terms, i.e.

$$\mu_1(X(t)) = \left(e^{-\left(\frac{|\nabla X(t)|^2}{k_1^2}\right)}, e^{-\left(\frac{|\nabla X(t)|^2}{k_2^2}\right)}\right) \text{ or }$$
 (3.17)

$$\mu_2(X(t)) = \left(\frac{1}{1 + \frac{|\nabla X(t)|^2}{k_1^2}}, \frac{1}{1 + \frac{|\nabla X(t)|^2}{k_2^2}}\right), \tag{3.18}$$

together with the Borkowski's diffusion term (2.4).

2. We consider (3.1) with Barbu's drift (2.2) and PM-functions for diffusion, terms i.e.

$$\sigma_1(X(t)) = \begin{pmatrix} -e^{-(\frac{|\nabla(G_{\gamma^*I})_y(X(t))|^2}{k_1^2})} & 0\\ -e^{-(\frac{|\nabla(G_{\gamma^*I})_x(X(t))|^2}{k_2^2})} & 0 \end{pmatrix} \text{ or }$$
(3.19)

$$\sigma_2(X(t)) = \begin{pmatrix} -\frac{1}{1 + \frac{|\nabla(G_{\gamma}*I)_{y}(X(t))|^2}{k_1^2}} & 0\\ \frac{1}{1 + \frac{|\nabla(G_{\gamma}*I)_{x}(X(t))|^2}{k_2^2}} & 0 \end{pmatrix},$$
(3.20)

with $k_1, k_2 \succ 0$.

- **3.** We consider (3.1) with (3.17) or (3.18) as drift term and $\sigma = 1$.
- **4.** We consider (3.1) with $\mu = 0$ and (3.19) or (3.20) for σ .

3.3. Mathematical analysis

3.3.1. Existence and Uniqueness

In this part, we investigate the well-posedness of the case 1 (i.e. a drift defined by (3.17) with Borkowski's diffusion (2.4)).

Theorem 3.5. Assume that all the conditions of Theorem 3.1 hold then (3.1) have a unique solution.

Proposition 3.6. Let μ_1 and σ be defined by (3.17) and (2.4), respectively, then

$$|\mu_1(t,X)| + |\sigma(t,X)| \le C_1(1+|X|), \quad C_1 > 0.$$
 (3.21)

Proof. We have μ and σ defined by (3.17) and (2.4), respectively

$$|\mu_1(t,X)|^2 = \left(e^{-\left(\frac{|\nabla X|^2}{k_1^2}\right)}\right)^2 + \left(e^{-\left(\frac{|\nabla X|^2}{k_2^2}\right)}\right)^2$$
< 2.

From (3.8), we have $|\sigma(t, X)| = 1$.

Hence

$$|\mu_1(t,X)| + |\sigma(t,X)| \le \sqrt{2} + 1.$$

This implies that there exists $C_1 > 0$ which satisfies the following relation

$$|\mu_1(t,X)| + |\sigma(t,X)| \le C_1(1+|X|), \quad C_1 > 0.$$
 (3.22)

So the condition (3.5) holds.

Proposition 3.7. Let μ_1 and σ defined by (3.17) and (2.4), then we have

$$|\mu_1(t,X) - \mu_1(t,Y)| + |\sigma(t,X) - \sigma(t,Y)| \le C_2|X - Y|. \tag{3.23}$$

Proof. If μ_1 and σ are given by (3.17) and (2.4), respectively, we write

$$|\mu_{1}(t,X) - \mu_{1}(t,Y)|^{2} = \left(e^{-\left(\frac{|\nabla X|^{2}}{k_{1}^{2}}\right)} - e^{-\left(\frac{|\nabla Y|^{2}}{k_{1}^{2}}\right)}\right)^{2}$$

$$+ \left(e^{-\left(\frac{|\nabla X|^{2}}{k_{2}^{2}}\right)} - e^{-\left(\frac{|\nabla Y|^{2}}{k_{2}^{2}}\right)}\right)^{2}$$

$$\leq \left(e^{-\left(\frac{|\nabla X|^{2}}{k_{1}^{2}}\right)}\right)^{2} + \left(e^{-\left(\frac{|\nabla Y|^{2}}{k_{1}^{2}}\right)}\right)^{2}$$

$$+ \left(e^{-\left(\frac{|\nabla X|^{2}}{k_{2}^{2}}\right)}\right)^{2} + \left(e^{-\left(\frac{|\nabla Y|^{2}}{k_{2}^{2}}\right)}\right)^{2}$$

$$\leq 4,$$

i.e.

$$|\mu_1(t, X) - \mu_1(t, Y)| \le 2.$$

In the same way we prove that

$$|\mu_1(t,X) - \mu_1(t,Y)| + |\sigma(t,X) - \sigma(t,Y)| \le C_2|X - Y|. \tag{3.24}$$

This yields that the proposed model (case 1) has a unique solution.

In the same way, we can demonstrate the existence and uniqueness of the solution for the other cases.

3.3.2. Numerical scheme

To discretize (3.1), we use Euler's numerical scheme and obtain

$$\begin{cases}
X_{t_{n+1}}^{m}(i,j) = X_{t_{n}}^{m}(i,j) + \Delta t \left(\mu(X_{t_{n}}^{m}(i,j)) + \sigma(X_{t_{n}}^{m}(i,j))(w_{i,j}^{n+1} - w_{i,j}^{n}) \right), \\
X_{0}^{m}(i,j) = X_{0}(i,j), i = \overline{1, M}, \ j = \overline{1, N},
\end{cases}$$
(3.25)

where $t_n = n\Delta t$, $\Delta t = \frac{T}{k}$, k = 0, 1, ..., m with k the number of t-iterations, and

$$w_{i,j}^n = w(n\Delta t, x_i, y_j),$$

with $x_i = i\Delta x$ and $y_j = j\Delta y$.

The drift and diffusion terms are approximated by

$$\mu(X_{t_n}^m(i,j)) = \begin{pmatrix} e^{-\left(\frac{(X_{n,i+1,j}^m - X_{n,i-1,j}^m)^2 + (X_{n,i,j+1}^m - X_{n,i,j-1}^m)^2}{4k^2}\right)} \\ \text{or} \\ \frac{1}{1 + \left(\frac{(X_{n,i+1,j}^m - X_{n,i-1,j}^m)^2 + (X_{n,i,j+1}^m - X_{n,i,j-1}^m)^2}{4k^2}\right)} \end{pmatrix},$$
(3.26)

and

$$\sigma(X_{t_n}^m(i,j)) = \begin{pmatrix} -\frac{(u_{i,j+1}^n + u_{i,j-1}^n) * 0.5}{\sqrt{\left(\frac{u_{i+1,j}^n + u_{i-1,j}^n}{2}\right)^2 + \left(\frac{u_{i,j+1}^n + u_{i,j-1}^n}{2}\right)^2}} & 0\\ \frac{(u_{i+1,j}^n + u_{i-1,j}^n) * 0.5}{\sqrt{\left(\frac{u_{i+1,j}^n + u_{i-1,j}^n}{2}\right)^2 + \left(\frac{u_{i,j+1}^n + u_{i,j-1}^n}{2}\right)^2}} & 0 \end{pmatrix},$$
(3.27)

here, the space steps $\Delta x = \Delta y = 1$, with

$$\begin{cases} (G_{\gamma} * u_0)_y = u_y = (u(i, j+1) + u(i, j-1)) * 0.5, \\ (G_{\gamma} * u_0)_x = u_x = (u(i+1, j) + u(i-1, j)) * 0.5. \end{cases}$$

3.4. Stability analysis

In this subsection, we present a numerical stability analysis for the numerical scheme (3.25).

Definition 3.8. Scheme (3.25) said to be stable, if there exists a constant C such that

$$|X_{t_{n+1}}^m(i,j) - X_{t_n}^m(i,j)| \le C\Delta t.$$
 (3.28)

Let us find the stability condition for (3.25), i.e. find C in (3.28) explicitly.

Proposition 3.9. If hypotheses (3.26) and (3.27) satisfy the properties of μ and σ , respectively, then

$$|X_{t_{n+1}}^m(i,j) - X_{t_n}^m(i,j)| \leq \Delta t \left(\sqrt{2} + \varepsilon_n(i,j)\right), \tag{3.29}$$

with $\varepsilon_n(i,j) > 0$.

Proof. To prove (3.28), we write

$$X_{t_{n+1}}^{m}(i,j) - X_{t_{n}}^{m}(i,j) = \Delta t \left[\mu(X_{t_{n}}^{m}(i,j)) + \sigma(X_{t_{n}}^{m}(i,j)) \cdot (w_{i,j}^{n+1} - w_{i,j}^{n}) \right], \tag{3.30}$$

we apply the Euclidean norm |.| on both sides of (3.30), to obtain

$$|X_{t_{n+1}}^{m}(i,j) - X_{t_{n}}^{m}(i,j)| = |\Delta t \left[\mu(X_{t_{n}}^{m}(i,j)) + \sigma(X_{t_{n}}^{m}(i,j))(w_{i,j}^{n+1} - w_{i,j}^{n})| \right]$$

$$\leq |\Delta t| \left[|\mu(X_{t_{n}}^{m}(i,j))| + |\sigma(X_{t_{n}}^{m}(i,j))| \right] \varepsilon_{n},$$
(3.31)

where

$$\varepsilon_n = \varepsilon_n(i,j) = |(w_{i,j}^{n+1} - w_{i,j}^n)|.$$

If we replace μ and σ by (3.26) and (3.27), respectively, we get

$$|\mu(X_{t_n}^m(i,j))| \le \sqrt{2},$$
 (3.32)

and

$$|\sigma(X_{t_n}^m(i,j))| = 1. \tag{3.33}$$

By substituting (3.32) and (3.33) in (3.31), we obtain

$$|X_{t_{n+1}}^m(i,j) - X_{t_n}^m(i,j)| \leq \Delta t \left(\sqrt{2} + \varepsilon_n(i,j)\right)$$

$$\leq C\Delta t \leq 1, \quad C > 0, \Delta t > 0,$$

leading to the following stability condition

$$\Delta t \le \frac{1}{C}, \ C = \sqrt{2} + \varepsilon_n(i, j) > 0, \tag{3.34}$$

for an appropriate choice of Δt to solve (3.25).

The other cases are proved in the same way.

4. Numerical Results and Comments

This section presents the numerical results and related comments. We consider a noisy image and apply the SDE models described in the previous sections, using different values for the variance γ .

First experimentations: we explored the following cases for $\gamma = 0.01$ and 0.1

- 1. PM-Borkowski: Borkowski's diffusion with PM-functions as drift term.
- 2. Barbu-PM: PM-functions as diffusion term and Barbu's drift term.
- 3. Barbu-Borkowski: Barbu's drift term and Borkowski's diffusion

Results are resumed in Table 1.

Second experimentations: we explored the following case for $\gamma = 0.01$

- C1 (Case 1): Barbu's drift with Borkowski's diffusion in (3.1).
- C2 (Case 2): PM-functions as a diffusion term with Barbu's drift.
- C3 (Case 3): Borkowski's diffusion with PM-functions as a drift term.
- C4 (Case 4): PM-functions as a diffusion term and drift term = 0.
- C5 (Case 5): PM-functions as a drift term with diffusion = 1.
- Kolmogorov PDE: Barbu's associated PDE [2] .

The obtained results are resumed in Table 2 & 3. and Figure 1 & 2.

Variance	Model	SSIM	PSNR	
0.1	Barbu	0.6257	23.6841	
	Borkowski	0.5302	22.9435	
	PM-Borkowski	0.7847	23.8949	
	Barbu-Borkowski	0.5754	23.0245	
	Barbu-PM	0.8014	24.5376	
0.01	Barbu	0.8755	30.6092	
	Borkowski	0.8557	30.2688	
	PM-Borkowski	0.9780	35.7153	
	Barbu-Borkowski	0.9051	32.1237	
	Barbu-PM	0.9871	38.6142	

Table 1: **PSNR** and **SSIM** values for different values of the variance with $\Delta t = 0.1$, T = 1.

Models	Barbu	Borkowski	C1	$C2 (\sigma_1)$	$C2 (\sigma_2)$	C3 (μ_1)
PSNR	30.6123	30.2688	32.2114	38.6125	38.5412	35.7283
SSIM	0.8746	0.8625	0.9022	0.9875	0.9820	0.9686
Models	C3 (μ_2)	$C4 (\sigma_1)$	$C4 (\sigma_2)$	C5 (μ_1)	C5 (μ_2)	PDE
PSNR	35.6909	29.2331	29.2691	29.8776	29.9572	23.0411
SSIM	0.9691	0.8488	0.8525	0.8688	0.8649	0.6511

Table 2: **PSNR** and **SSIM** values using different approaches for $\gamma = 0.01$, $\Delta t = 0.1$, T = 1, M = 12.

Models	PM 1	PM 2	Barbu	Borkowski	C1	$C2 (\sigma_1)$	$C2 (\sigma_2)$
PSNR	27.4508	27.6078	30.6202	30.1778	32.1417	38.5159	38.6181
SSIM	0.8580	0.8608	0.8743	0.8735	0.9854	0.9869	0.9779
Models	C3 (μ_1)	C3 (μ_2)	$C4 (\sigma_1)$	$C4 (\sigma_2)$	C5 (μ_1)	C5 (μ_2)	PDE
PSNR	35.7369	35.7744	29.4182	29.2514	29.8761	29.7959	23.1026
SSIM	0.8685	0.8695	0.8520	0.8486	0.8675	0.8635	0.6562

Table 3: **PSNR** and **SSIM** values using different approaches for $\gamma = 0.01$, $\Delta t = 0.5$, T = 10, M = 12

4.1. Comments

In this section, we compare the obtained numerical results. We applied the proposed model (3.1) with different expressions for diffusion σ and drift μ terms. The discretisation parameters used for our numerical implementations are, stopping time T=1 & 10, step time $\Delta t=0.1$ & 0.5, number of iterations M=12, $\alpha_1=2$, $\alpha_2=4$, $k_1=20$ and $k_2=40$.

As illustrated in Tables 1., 2. & 3., and Figure 1. & 2., we note that the proposed models ((3.1) together with (3.17) or (3.18), (3.19) or (3.20)) exhibit strong performance in both noise removal and the preservation of essential image features (such as edges, texture, curvature, etc..), compared to the combined Barbu-Borkowski SDE (Borkowski's diffusion and Barbu's drift terms). The two cases are largely comparable; however, the results obtained in the second case where Barbu's drift and Perona-Malik functions are used for the drift and diffusion terms, respectively offer a modest enhancement over those of the first case.

Table 1., 2 & 3. and Figure 1. & 2. give the numerical findings in terms of the Peak Signal to Noise Ratio (DSNR) and Structure Similarity Index Margues (SSIM) are a greened a nitrous that has been used if add here.

Table 1., 2 & 3. and Figure 1. & 2. give the numerical findings in terms of the Peak Signal to Noise Ratio (PSNR) and Structure Similarity Index Measure (SSIM) on a greyscale picture that has been modified by Gaussian white noise with a mean of zero and variance of $\gamma = 0.1$ & 0.01.

We have studied a comparison of the 5 cases for (3.1), and conclude that: - All SDEs cases give better results compared to PDEs based models.

- Case 2 ($\sigma_1 \& \sigma_2$) provides the best performance, demonstrating both strong numerical accuracy and excellent structural preservation compared to the other models.
- Case 1 achieves competitive results, outperforming Barbu's and Borkowski's models, although its performance remains below that of case 2.
- Case 3 (μ_1 & μ_2) yields improved results over Cases 1, 4, and 5, highlighting the suitability of the chosen drift and diffusion terms.
- Cases 4 & 5, are explored in a such way that PM-functions are used either for the diffusion or drift terms together with the Barbu's drift (2.1) and Borkowski's diffusion (2.3). In order to extract the inconveniences of these models when neglecting one of the terms, we note that we get better values for PSNR and SSIM.

We have to point out that:

- 1- if we investigate numerically for larger time T, we obtain the same qualitative results but with more t-iterations, see results in Table 2. & 3.
 - 2- The number of Monte Carlo iterations is related to the trajectories computation not the solution.
- 3- Other numerical experimentations have been carried out on a medical image and results are shown in Figure 2.

5. Conclusion

In this work, we proposed a model that uses stochastic processes to restore images. The use of both terms (drift and diffusion) in SDE (3.1) aims to eliminate noise without sacrificing essential features or introducing false ones. The diffusion and drift terms have been adapted to better reflect the complexity of

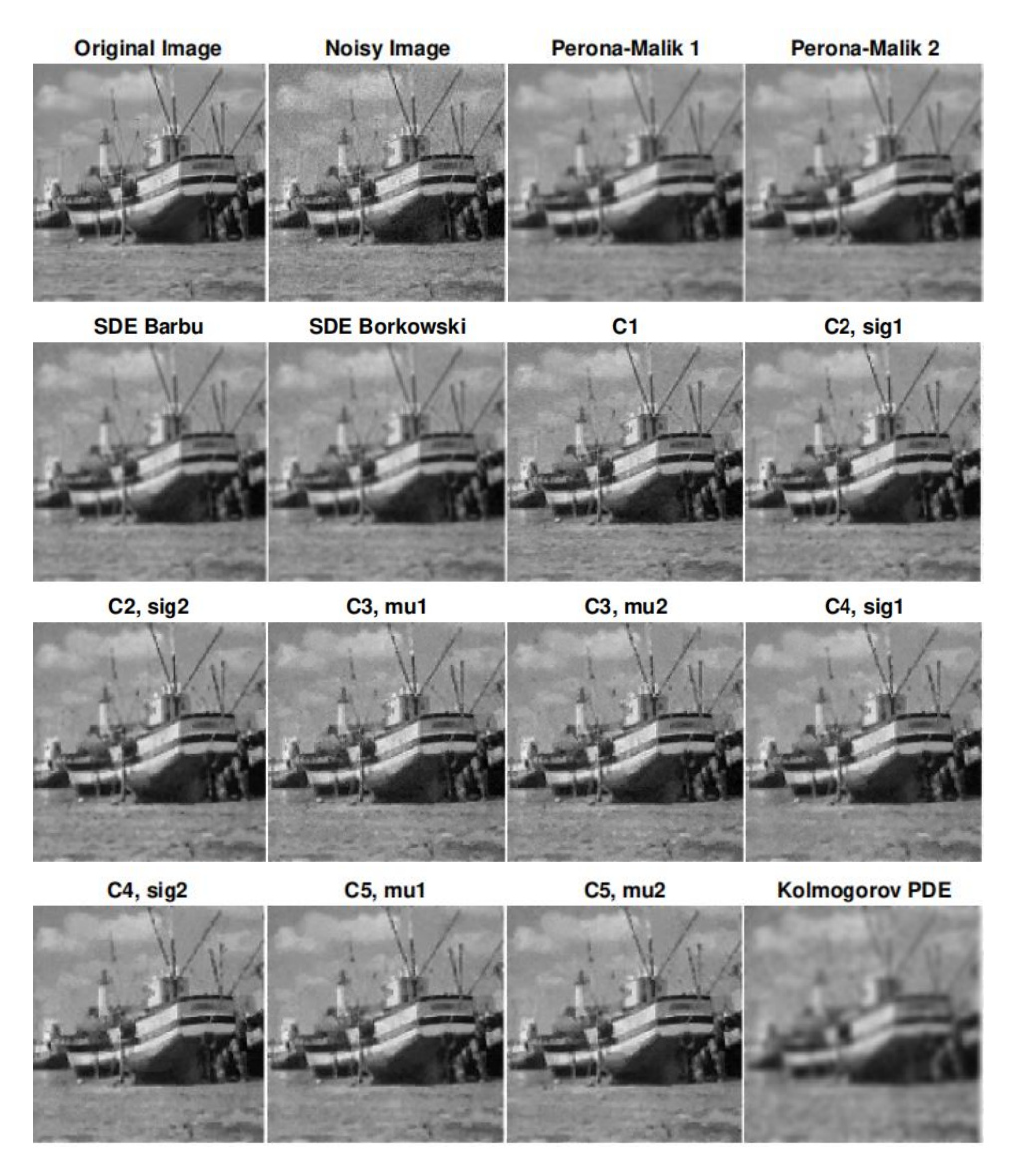


Figure 1: Restored image results for the different cases with $\Delta t = 0.1$, $\gamma = 0.01$, T = 1, M = 12.

the geometric structures. Based on the numerical results obtained, we conclude that, in comparison to the combined Barbu-Borkowski SDE, our proposed models are generally more qualitatively efficient. This can be observed both visually, as in Figure 1 and 2, and quantitatively through the PSNR and SSIM metrics, as shown in Tables 1, 2 and 3. It is worth noting that the proposed models are also more intuitively realistic, producing encouraging numerical results in terms of noise removal and feature preservation when compared to PDE-based models. Furthermore, these models can be very promising for image inpainting [3] and [18].

References

- [1] T. Barbu, G. Da Prato and L. Tubaro, Kolmogorov equation associated to the stochastic reflection problem on a smooth convex set of a Hilbert space II, Annales de l'IHP Probabilités et Statistiques, (2011) 699-724. (document), 1
- [2] T. Barbu and A. Favini, Novel stochastic differential model for image restoration, Proceedings of the Romanian Academy-Series A: Mathematics, Physics, Technical Sciences, Information Science, (2016) 109-116. (document), 1, 2.1, 4
- [3] M. Benseghir and F.Z. Nouri, A new partial differential equation for image inpainting, Bol. Soc. Paran. Mat. (2021) 137-155. 5

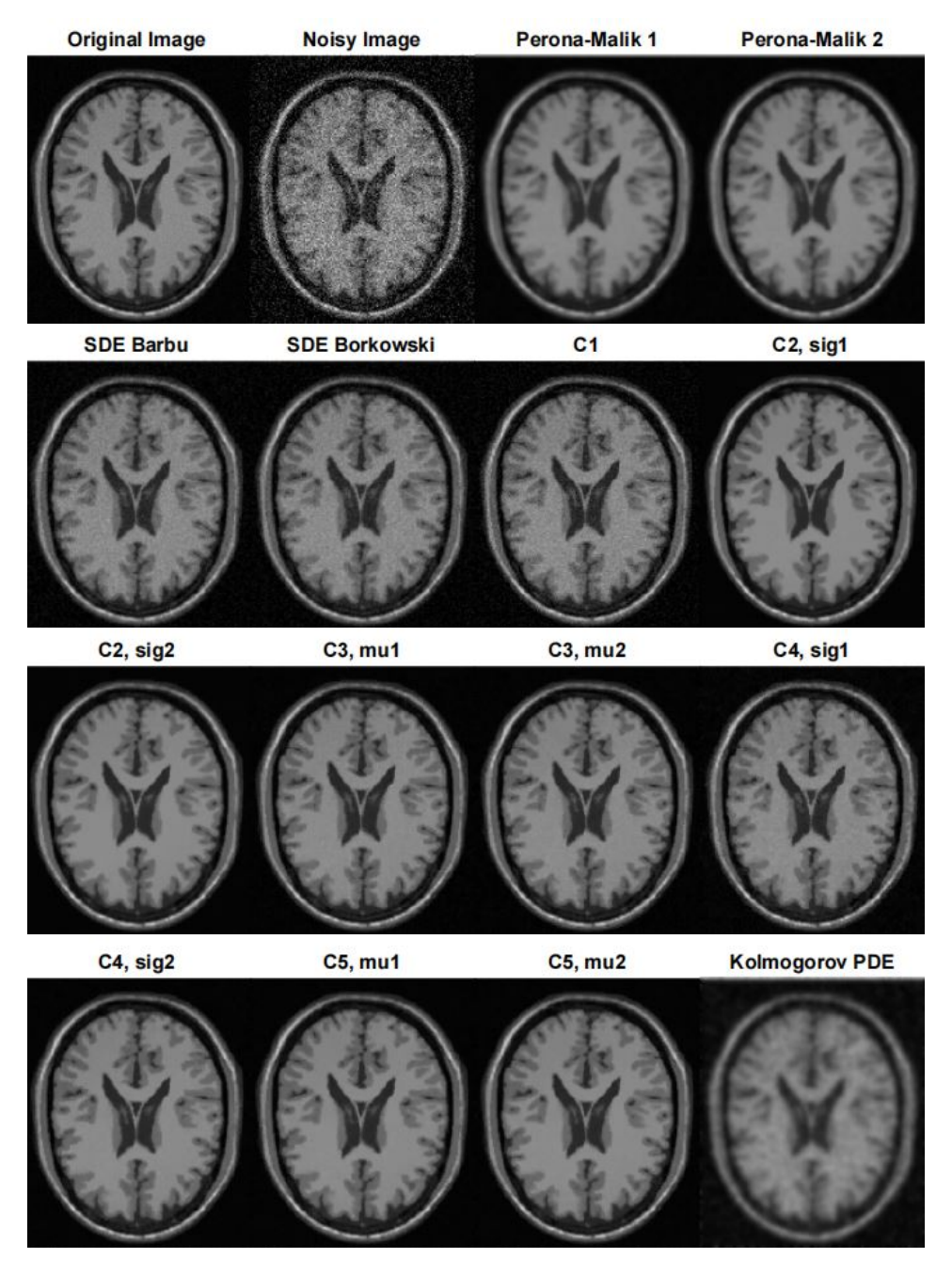


Figure 2: Restored image results for the different cases with $\Delta t = 0.5$, $\gamma = 0.01$, T = 10, M = 12

- [4] D. Borkowski and K.J. Borkowska, Image restoration using anisotopic stochastic diffusion collaborated with non local means, In IFIP Internatinal Conference on Computer Information Systems and Industial Management, Krakow, Poland (2013) 177-189. (document), 1, 2.2
- [5] D. Borkowski, Forward and backward filtering based on backward Stochastic differential equations, Inverse Problems and Imaging, (2016) 305-325. 1
- [6] D. Borkowski and K.J. Borkowska, Image denoising using backward stochastic differential equations, Advances in Intelligent Systems and Computing, (2017) 185-194.
- [7] K. Dabov, A. Foi, V. Katkovnik and K. Egiazarian, Image denoising by sparse 3D transform-domain collaborative filtering, IEEE Transactions on Image Processing, (2007), 2080-2095. 1
- [8] X. Descombes and E. Zhizhina, Image denoising using stochastic differential equations, INRIA, (2003), 1-30. 1
- [9] X. Descombes, M. Lebellego and E. Zhizhina, Image deconvolution using a stochastic differential equation approach, In Proceedings of The Second International on Computer Vision Theory and Applications, (2007) 157-164.

- [10] M. Diwakar and M. Kumar, A review on CT image noise and its denoising, ELSEVIER, Biomedical Signal Processing and Control, (2018) 73-88. 1
- [11] L. Fan, F. Zhang, H. Fan and C. Zhang, Brief review of image denoising techniques, Visual Computing for Industry, Biomedicine, and Art, Springer Open, (2019), 1-12. 1
- [12] H.T. Huynh, V.S. Lai, I. Soumaré, Stochastic simulation and applications in finance with matlab, John Wiley & Sonc. 2008. 1
- [13] Y. Jiang Li, J. Zhang and M. Wang, Improved BM3D denoising method, IET Image Processing, (2017) 1197-1204.
- [14] S. Kichenassamy, A. Kumar, P. Olver, A. Tannenbaum and A. Yezzi, Jr, Conformal curvature flows: From phase transitions to active vision. Arch. Rational Mech. Anal. (1996) 275-301.
- [15] Jan J. Koendrink, The structure of images, Biol. Cybern (1984) 363-370. 1
- [16] S. Kumar Maji, R.K. Thakur and H.M. Yahia, SAR image denoising based on multifractal feature analysis and TV regularisation, IET Image Processing, (2020), 1-10. 1
- [17] J.M. Morel and Rudin-Osher-Fatemi, Total variation denoising using split bregman, Image Processing On Line, Pascal Getreuer, (2012) 74-95. 1
- [18] F.Z. Nouri, Uniqueness and Existence Results for a partial Differential Equation in Image Inpainting, Commun. Optim. Theory 2020 (2020) Article ID7 1-17. https://doi.org/10.23952/cot.2020. 1, 5
- [19] B. Øksendal, Stochastic differential equations, Universitext, Springer, (Sixth Edition), 2013. 1, 3.1
- [20] P. Perona and J. Malik, Scale-space and edge detection using anisotropic diffusion, IEEE Trans. Pattern Anal. Machine Intell., (1990) 629-639. 1
- [21] E.H. Soubari, Traitement d'images par transformer de Fourier optique, Departement Des Arts Graphiques, B.P. 6009-45060 Orléans Cédex, (1979), 1-40. 1
- [22] N. Touzi, EDS retrogrades et EDP non lineaires, Conférence de la SMAI sur l'optimisation et la décision, Ecole Polytechnique, (2007). 1
- [23] S.J. Walker, Fourier analysis and wavelet analysis, Notices of The AMS, (1997) 658-670. 1
- [24] Y. Wang, G. Wei Wei and S. Yang, Partial differential equation tronsform variational formulation and Fourier Analysis, Int. J. Numer. Meth. Biomed. Engng. (2011), 1-25.
- [25] J. Weickert, Anisotropic diffusion in image processing, Teubner, (1998). 1
- [26] J. Weickert, T. Brox, B. Burgeth and Pavel Mràzek, Nonlinear structure tensors, Image and Vision Computing, (2006) 41-55. 1
- [27] J. Weickert, T. Brox, Diffusion and regularization of vector-and matrix-valued images, Saarbrucken (2002) 251-268. 1